Plant Physiol. (1998) 117: 345–361

Temporal Sequence of Cell Wall Disassembly in Rapidly Ripening Melon Fruit[1]

Jocelyn K.C. Rose, Kristen A. Hadfield, John M. Labavitch, and Alan B. Bennett*

Mann Laboratory, Department of Vegetable Crops (J.K.C.R., K.A.H., A.B.B.), and Department of Pomology (J.M.L.), University of California, Davis, California 95616

The Charentais variety of melon (*Cucumis melo* cv Reticulatus F1 Alpha) was observed to undergo very rapid ripening, with the transition from the preripe to overripe stage occurring within 24 to 48 h. During this time, the flesh first softened and then exhibited substantial disintegration, suggesting that Charentais may represent a useful model system to examine the temporal sequence of changes in cell wall composition that typically take place in softening fruit. The total amount of pectin in the cell wall showed little reduction during ripening but its solubility changed substantially. Initial changes in pectin solubility coincided with a loss of galactose from tightly bound pectins, but preceded the expression of polygalacturonase (PG) mRNAs, suggesting early, PG-independent modification of pectin structure. Depolymerization of polyuronides occurred predominantly in the later ripening stages, and after the appearance of PG mRNAs, suggesting the existence of PG-dependent pectin degradation in later stages. Depolymerization of hemicelluloses was observed throughout ripening, and degradation of a tightly bound xyloglucan fraction was detected at the early onset of softening. Thus, metabolism of xyloglucan that may be closely associated with cellulose microfibrils may contribute to the initial stages of fruit softening. A model is presented of the temporal sequence of cell wall changes during cell wall disassembly in ripening Charentais melon.

Ripening in many fruits is associated with textural changes that are believed to result from disassembly of the primary cell wall. This includes modifications of the structure and composition of the constituent polysaccharides that have been correlated with the expression of a range of hydrolases and transglycosylases (Fischer and Bennett, 1991; Lashbrook et al., 1997) and the potential alteration of covalent and noncovalent interactions between polysaccharide classes. A recent model of the plant primary cell wall described a network of cellulose microfibrils that surrounds the cell and is enmeshed in coextensive matrices of pectic and hemicellulosic polymers, with additional minor components such as structural proteins (Carpita and Gibeaut, 1993). During fruit softening, pectins (Brady, 1987; Fischer and Bennett, 1991) and hemicelluloses (Lashbrook et al., 1997) typically undergo solubilization and depolymerization that are thought to contribute to wall loosening and disintegration, although the relative extent and timing vary between species.

Extensive research has addressed the cell wall changes that occur in ripening tomato fruit, and many reports have focused on the considerable pectin degradation that coincides with softening and expression of the pectin hydrolase PG (Huber, 1983; Hobson and Grierson, 1993). Early models implied that PG-catalyzed pectin degradation represented the fundamental process underlying fruit softening (Crookes and Grierson, 1983); however, molecular genetic approaches subsequently revealed that PG-dependent pectin degradation is not essential for fruit softening (Smith et al., 1988; Giovannoni et al., 1989), but may play a role in other aspects of fruit quality (Kramer et al., 1990; Schuch et al., 1991). This suggests that other wall polymers contribute significantly to fruit firmness, and recent studies have examined the extent of hemicellulose degradation during fruit ripening (for review, see Lashbrook et al., 1997). The principal hemicellulose in dicotyledons is xyloglucan, and it has been demonstrated that xyloglucan undergoes substantial depolymerization in many ripening fruit, including tomato (Sakurai and Nevins, 1993; Maclachlan and Brady, 1994).

Xyloglucan coats and cross-links cellulose microfibrils (Hayashi and Maclachlan, 1984; McCann et al., 1990), and disruption of the cellulose/xyloglucan matrix may be a key element in regulating wall integrity. Additional hemicellulosic polymers, including xylans, arabinoxylans, mannans, and galactoglucomannans, have been detected in different fruit species; however, these are typically minor components and turnover of these polysaccharides during ripening remains relatively unexplored.

In addition to the depolymerization of both pectic and hemicellulosic polymers, a characteristic feature of ripening fruit is the loss of neutral sugars from the cell wall, primarily Gal and Ara (Gross and Sams, 1984). This has been associated with a decrease in neutral sugar concentration of both pectic and hemicellulosic polysaccharides (Gross and Wallner, 1979; McCollum et al., 1989; Kojima et al., 1994), although this and the relative extent of neutral sugar loss appear to vary between species.

Tomato has served as a model for cell wall disassembly during ripening because of the extensive literature related to modification of polysaccharide structure and composi-

[1] This research was supported by a grant from Zeneca Plant Science, Jealotts' Hill, UK.

* Corresponding author; e-mail abbennett@ucdavis.edu; fax 1–530–752–4554.

Abbreviations: AIS, alcohol-insoluble solids; CDTA, cyclohexane diamine tetraacetic acid; DAP, days after pollination; IG, immature-green ripening stage; MG, mature-green ripening stage; PG, polygalacturonase; R1 to R4, ripening stages 1 to 4; Rha, rhamnose; TS, total sugars; UA, uronic acid.

tion, and because there are several ripening mutants that can exhibit dramatically reduced softening and have therefore been used as genetic tools to investigate ripening-related processes (Ng and Tigchelaar, 1977; Mitcham et al., 1991; Maclachlan and Brady, 1994). Tomato fruit, however, generally develop from the preripe to the overripe stage over a period of approximately 10 to 18 d, depending on the variety. In contrast, fruit of the Charentais variety of melon (*Cucumis melo* cv Reticulatus F1 Alpha) undergo remarkably rapid softening; vine-ripened fruit typically undergo an equivalent transition from the preripe to overripe stages in 24 to 48 h. Therefore, Charentais melons may represent an excellent model system in which to examine the temporal sequence of cell wall disassembly.

The rapid softening of Charentais melons also raised the question of whether it involved characteristic wall modifications that have been reported in other fruit (including other melon varieties; Lester and Dunlap, 1985; McCollum et al., 1989), but at a much accelerated rate, or whether a unique pattern of wall degradation exists in this variety. Furthermore, the large fruit provide an abundant source of material at a uniform stage of development for extraction of substantial quantities of cell wall material, nucleic acids, and protein from a single fruit.

We describe the process of wall disassembly in ripening Charentais fruit in terms of cell wall composition and degradation of hemicellulosic and pectic polymers, and identify features that are associated with early and later stages of melon fruit softening.

MATERIALS AND METHODS

Charentais melon (*Cucumis melo* cv Reticulatus F1 Alpha) flowers were tagged on the day of pollination and a developmental series of fruit was subsequently harvested at defined DAP or at specified ripening stages: IG, attaining full size between 20 and 26 DAP; MG, full size between 30 and 34 DAP, pale green rind, and no detectable internal ethylene or discernible softening; R1, the onset of ripening with detectable levels of ethylene production and $<$ 10% loss of flesh firmness; R2, approximately 30% loss of flesh firmness, 10 to 30 μL L^{-1} internal ethylene; R3, 50 to 75% of maximal softening, internal ethylene concentration in excess of 80 μL L^{-1}; and R4, overripe, orange rind, disintegrated and waterlogged flesh, and fruit often split open at the blossom end. The internal concentration of ethylene was determined with the fruit attached to the vine, as described in Hadfield et al. (1995). Equatorial sections were cut from the fruit and the flesh firmness was measured at points 2 cm from the junction of the rind and the outer pericarp using a 0.8-mm-diameter probe attached to a firmness tester penetrometer (Western Industrial Supply, San Francisco, CA). The flesh was then frozen in liquid N_2 and stored at -80°C.

Isolation of Cell Walls and Determination of Autolytic Activity

Approximately 50 g of frozen outer pericarp tissue from each fruit developmental stage was boiled with 250 mL of 95% ethanol for 30 to 45 min, homogenized in a blender (Waring), and filtered through Miracloth (Calbiochem). Insoluble material was washed sequentially with 500 mL of boiling ethanol, 500 mL of chloroform:methanol (1:1, v/v), and 500 mL of acetone; oven-dried at 30°C; and stored in an auto-desiccator (RPI, Mount Prospect, IL), yielding the crude cell wall extract, alcohol insoluble solids. Subsequent assessment of autolytic activity of the samples and sequential chemical extraction are described below and shown in Figure 1.

A variety of protocols for isolating autolytically inactive cell wall material have been developed that rely on phenol-acetic acid:water (2:1:1, v/v) or Tris-buffered phenol to inactivate endogenous cell wall-bound enzymes (Huber, 1992; Redgwell et al., 1992; Huber and O'Donohue, 1993). Other reports have found that extraction of tissue in boiling ethanol can successfully prevent the autolytic generation of reducing end groups during subsequent experiments with AIS preparations (Carrington et al., 1993). The AIS residue isolated from melon, described above, was assayed for autolytic activity to confirm the effectiveness of the ethanol extraction in providing autolytically inert material. Approximately 30 mg of AIS from both R1 and R4 stages was resuspended in 5 mL of 40 mM $NaC_2H_3O_2$, pH 5.0, several drops of toluene were added, and the mixture was incubated at 30°C for up to 24 h. As a control, identical experiments were performed using pericarp tissue homogenized in 40 mM $NaC_2H_3O_2$, pH 5.0, or in ethanol at room temperature.

Aliquots (250 μL) were extracted over the 24-h time course, passed through 0.45-μm filters (Uniflo, Schleicher & Schuell), and assayed for TS using the phenol-sulfuric acid method (Dubois et al., 1956). Whereas a linear increase in the solubilization of TS from the buffer-homogenized material was observed over 24 h, a minimal release (ap-

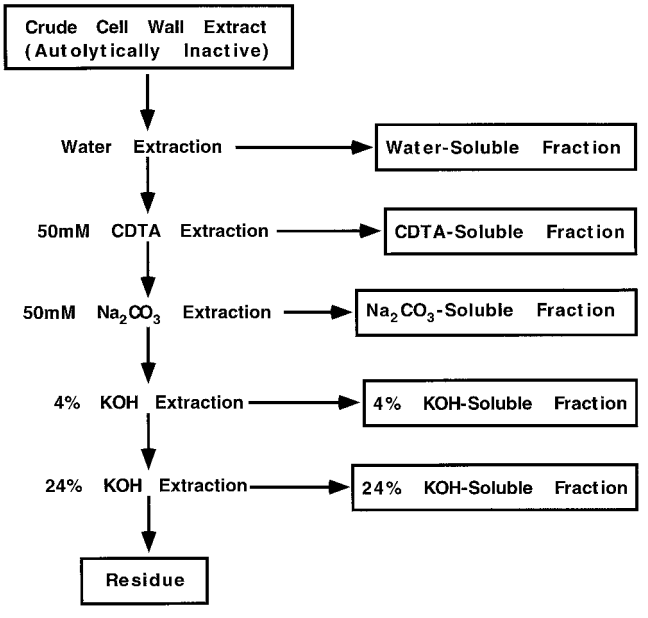

Figure 1. Sequential chemical-extraction protocol used for the preparation and isolation of Charentais melon fruit cell wall fractions.

proximately 8-fold less) was detected from room-temperature-ethanol-extracted AIS, and no increase was detected from boiling-ethanol-extracted cell wall material (data not shown). It was concluded that the melon AIS isolated using boiling ethanol was autolytically inactive.

Cell Wall Chemical Extraction and Fraction Analysis

The AIS residue from each sample was homogenized in 75 mL of 0.02% NaN_3 for 4 h at room temperature and centrifuged at 6,000*g* for 20 min, and the pellet was extracted twice with 25 mL of 0.02% NaN_3 for 20 min. The supernatants were combined, lyophilized, resuspended, and stirred in 15 mL of DMSO:water (9:1, v/v) for 24 h to solubilize any starch (although it has been reported that melons accumulate little, if any, starch [Pratt, 1971]), and then centrifuged at 20,000*g* for 20 min and filtered through Miracloth (Calbiochem). The pellet was washed with 50 mL of DMSO:water, followed by three washes with 30 mL of 80% ethanol and three washes with 30 mL of acetone, oven-dried at 30°C, and stored in a desiccator. This was designated the water-soluble fraction. Aliquots of the supernatants from the DMSO extraction were combined with 2 volumes of ice-cold 95% ethanol to precipitate polymeric material, stirred at 1°C for 12 h, centrifuged at 6,000*g* for 30 min, and filtered, and any pelleted material was washed with 150 mL of ice-cold 95% ethanol. Virtually no polysaccharide was extracted with DMSO from any developmental stage, and analysis of the sugar composition of any detectable pellet by GC (for methodology, see below) showed a ratio of neutral sugars similar to that of the total water-soluble fraction, indicating that differential solubilization of specific cell wall polymers by DMSO had not occurred.

The water-insoluble pellets were homogenized with 50 mM CDTA and 50 mM $NaC_2H_3O_2$, pH 6.5, stirred vigorously at room temperature for 12 h, filtered and centrifuged as for the water-soluble fraction, and re-extracted with an additional 50 mL of the same solution for 12 h. The supernatants were combined and exhaustively dialyzed (M_r cut-off 6–8 kD) against distilled water for 2 d at 5°C, lyophilized, and stored in a desiccator. The CDTA-insoluble pellet was washed once with 50 mL of the CDTA buffer solution, twice with 100 mL of 80% ethanol, and twice with 100 mL of acetone, and was then extracted with 50 mL of 50 mM Na_2CO_3 and 20 mM $NaBH_4$ at 1°C as for the CDTA extraction. The 4 and 24% KOH fractions were obtained by sequential chemical extraction of Na_2CO_3-insoluble material, as described in Maclachlan and Brady (1994).

Samples of the crude cell wall (AIS) and sequentially extracted fractions were assayed for total UA (Ahmed and Labavitch, 1977) and TS using a modification of the phenol-sulfuric acid assay (Dubois et al., 1956), in which the lyophilized sample was first dissolved in sulfuric acid/water as for the UA assay above. Aliquots were removed and the reagents for the phenol-sulfuric acid assay added in the following order: sulfuric acid, phenol, and water, using Glc as a standard. For GC analysis of the AIS and extracted fractions, aliquots were hydrolyzed with 2 N trifluoroacetic acid at 121°C for 1 h, and the resulting hydrolysates were converted to alditol acetates (Blakeney et al., 1983). Analysis of neutral sugar composition used a gas chromatograph (model 8320, Perkin-Elmer) with a 30-m × 0.25-mm i.d. capillary column (model DB-23, J & W Scientific, Folsom, CA) as described in Carrington et al. (1993).

Size-Exclusion Chromatography and Analysis of Subfractions

Aliquots (approximately 5 mg) of lyophilized water-, CDTA-, or Na_2CO_3-soluble polymers were chromatographed on a size-exclusion column (1.0 × 90 cm) of Sepharose CL-4B (Pharmacia) eluted in 200 mM NH_4-acetate, pH 5.0. Fractions were collected (2.0 mL) at a flow rate of 17 mL h^{-1} and assayed for UA by the *m*-hydroxydiphenyl method (Blumenkrantz and Asboe-Hansen, 1973) and for TS as described in Dubois et al. (1956). Although the NH_4-acetate buffer has been reported to reduce aggregation of pectins during chromatography (Mort et al., 1991), it was observed to cause interference with the UA assay. This was avoided by leaving the fractions at room temperature for 48 to 72 h before analysis, presumably allowing a portion of the buffer to volatilize.

Size separation of 4 and 24% KOH-soluble polymers was with a Sepharose CL-6B column (1.0 × 90 cm, Pharmacia) eluting with 0.1 N NaOH. Aliquots of lyophilized extract (2.0 mg) were applied to the column and 2-mL fractions were collected at a flow rate of 18 mL h^{-1}, neutralized with glacial acetic acid, and assayed for TS as above or for xyloglucan as described in Maclachlan and Brady (1994). For neutral sugar compositional analysis, subfractions were pooled, lyophilized, washed with 20 mL of ice-cold 95% ethanol to reduce the salt concentration, lyophilized again, and then the component sugars were hydrolyzed, derivitized to alditol acetates, and analyzed by GC as described above.

RESULTS AND DISCUSSION

Correlation of Flesh Softening with Internal Ethylene Concentration

The large central cavity in Charentais melons allows sampling and accurate determination of internal gas concentrations with no apparent disturbance to normal fruit development. Using such techniques it has previously been reported that Charentais melons exhibit a respiratory climacteric during ripening that coincides with an abrupt increase in internal ethylene concentration (Hadfield et al., 1995). Figure 2 shows a typical profile of increasing internal ethylene concentration concomitant with a loss of flesh firmness during ripening. No substantial softening was observed between IG and R1. Rapid loss of firmness was initiated at R1, corresponding to the first detectable rise in internal ethylene, and this trend continued through R4.

Over the course of three seasons, it was observed that the fruit did not ripen synchronously, based on the number of DAP, but that individual fruit typically made the transition from MG to R4 within 24 to 48 h. Similarly, a dramatic loss

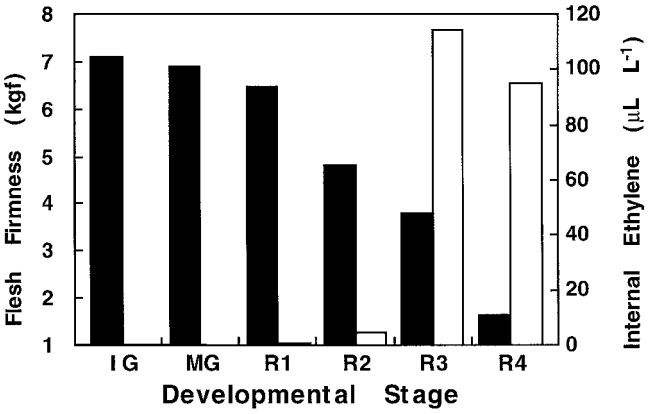

Figure 2. Flesh firmness (black bars) and internal ethylene concentration (white bars) of Charentais melon fruit at defined developmental stages. kgf, Kilograms force.

of firmness was observed 24 to 48 h following treatment of preripe fruit with ethylene (data not shown). As described in "Materials and Methods," the fruit shown in Figure 2 were defined based on representative stages of development for these experiments, rather than on DAP. As far as we are aware, softening of vine-ripened Charentais melon fruit occurred more rapidly than has been reported for any other species to date, and therefore represent an excellent system in which to examine the temporal sequence of cell wall modification. Furthermore, the large fruit size allowed the use of a series of individual fruit at characterized uniform developmental stages as sources of cell wall material.

Yield and Composition of Cell Wall Fractions

Autolytically inactive crude cell wall extracts, termed AIS, were assayed for both UA and TS content and then subjected to sequential chemical extraction (Fig. 1) designed to enrich for particular subclasses of cell wall polymers. The water-soluble fraction is typically thought to include polymeric material that has been solubilized from the cell wall, whereas the CDTA- and Na_2CO_3-soluble fractions are generally considered to be enriched for ionically and covalently bound pectins, respectively. Polymers extracted with 4% KOH usually contain a high proportion of hemicellulosic polysaccharides, whereas 24% KOH is necessary to extract hemicellulose-rich polymers that are tightly bound to the cell wall, and to cellulose microfibrils in particular. The residual material following 24% KOH extraction is comprised of mainly cellulose and a small quantity of associated polysaccharides. The total mass of AIS extracted from different ripening stages did not change and comprised about 1.5% of the fresh weight of the fruit. Fractions derived from the AIS were also assayed for UA and TS (Table I).

GC analysis of the noncellulosic neutral sugar composition of both the AIS and wall fractions (Table II) was used to determine whether changes in the proportion of specific sugars could be correlated with early or late stages of softening, and to provide a basis for association of particular classes of polysaccharide with specific ripening stages or cell wall fractions.

Yield and Composition of Pectic Fractions

In common with previous analyses of other melon varieties (McCollum et al., 1989; Simandjuntak et al., 1996), the total polyuronide content of the cell wall showed little change either prior to or during ripening. However, there was a substantial change in the relative solubility of pectins among the cell wall fractions as softening proceeded (Table I). At the IG stage only 19% of the total UA was water soluble, whereas the CDTA- and Na_2CO_3-soluble fractions together accounted for 66% of the total polyuronides. The relative proportion of pectins among these three fractions showed little change between IG and R1, although there was a small increase in the UA content of the Na_2CO_3-soluble fraction and a corresponding decrease in the CDTA-soluble fraction.

Between R1 and R2, an increase in the proportion of CDTA-soluble pectins was accompanied by a marked reduction in Na_2CO_3-soluble UA, which then decreased even more substantially between R2 and R3. The quantity of water-soluble UA increased at R3 and again to a greater extent between R3 and R4, when it comprised 40% of the total AIS. Similar losses of polyuronides were detected in the 4 and 24% KOH-soluble fractions between R2 and R3, although these comprised less than 6% of the total AIS UA. Small quantities of polyuronides were detected in the residual cell wall material, but the relative amounts did not change during ripening.

Assay of TS using the phenol-sulfuric acid method is primarily to quantify noncellulosic neutral sugars, although there is a low degree of sensitivity to galacturonosyl residues, and this was used to monitor TS in the cell wall fractions. TS was relatively consistent through the R1 stage (Table I), followed by a consistent decline at the onset of softening between R1 and R4. The relative amount of TS in the water- and Na_2CO_3-soluble fractions was greater than that in the CDTA-soluble fraction and showed changes similar to those of UA, increasing and decreasing in the later ripening stages, respectively. The ratio of TS to UA was considerably greater in the Na_2CO_3-soluble fraction than in the CDTA-released polymers (1:1.2 and 1:5.3 at IG, respectively), suggesting a greater degree of branching and neutral sugar substitution of the covalently bound pectins. A high ratio of neutral sugar to UA in the Na_2CO_3-soluble polymers suggests an origin in the primary cell wall, whereas a low ratio in the CDTA-extracted fraction is indicative of pectins from the middle lamella, as has been reported in other species (Seymour et al., 1990; Cutillas-Itturralde et al., 1993). No changes in the relative proportion of TS were apparent during ripening in the CDTA-soluble fraction.

Analysis of the noncellulosic neutral sugar composition of the AIS (Table II) revealed that the predominant neutral sugar was Gal at all stages, although a 27% decrease of the Gal mol % concentration occurred between the IG and R4 stages. Similarly, the concentration of Ara decreased by 31% over the same developmental period. Conversely, the

Table I. *TS and UA distribution among melon cell wall-polymer fractions*

Fraction	Stage	UA	UA in AIS	TS[a]	TS in AIS[a]
		μg mg⁻¹ AIS	*% total*	*μg mg⁻¹ AIS*	*% total*
Crude cell wall (AIS)	IG	335	N/A[b]	602	N/A
	MG	317	N/A	644	N/A
	R1	346	N/A	609	N/A
	R2	329	N/A	581	N/A
	R3	315	N/A	526	N/A
	R4	295	N/A	491	N/A
Water-soluble	IG	63	19	69	12
	MG	69	22	75	12
	R1	62	18	84	14
	R2	68	21	72	12
	R3	86	27	87	17
	R4	118	40	106	22
CDTA-soluble	IG	106	32	20	3
	MG	92	29	24	4
	R1	96	28	28	5
	R2	130	40	39	7
	R3	138	44	27	5
	R4	130	44	25	5
Na_2CO_3-soluble	IG	113	34	94	16
	MG	128	40	82	13
	R1	137	40	86	14
	R2	107	33	88	15
	R3	43	14	63	12
	R4	39	13	31	6
4% KOH-soluble	IG	10	3	92	15
	MG	9	3	104	16
	R1	11	3	112	18
	R2	10	3	109	19
	R3	5	2	77	15
	R4	6	2	81	16
24% KOH-soluble	IG	7	2	186	31
	MG	6	2	182	28
	R1	5	1	164	27
	R2	7	2	166	29
	R3	4	1	152	29
	R4	2	1	150	31
Residue	IG	19	6	98	16
	MG	12	4	111	17
	R1	11	3	152	25
	R2	20	6	126	22
	R3	22	7	128	24
	R4	16	5	122	25

[a] Measured in Glc equivalents. [b] N/A, Not applicable.

mol % of Xyl increased primarily in the later ripening stages, whereas Glc increased from IG to R2 and decreased between R2 and R3. The loss of Gal and Ara from the AIS is typical of many fruit species and has been reported in other melon varieties (Gross and Sams, 1984; McCollum et al., 1989; Simandjuntak et al., 1996), although the polymeric origin has not been investigated and these sugars are constituents of both hemicelluloses and pectins.

The pectin-rich (water-, CDTA-, and Na_2CO_3-soluble) fractions contained a high proportion of Ara and Gal. In the water-soluble fraction, Ara and Gal showed opposite patterns of relative abundance, increasing and decreasing, respectively, in the later softening stages. In the water-soluble polymers, as in the CDTA-soluble fraction and the AIS, Glc showed a transient increase from 11.6 mol % at IG to 13.7 mol % at R1, before declining to comprise only 8 mol % at R4. Glc, if present, is considered to be only a minor component of pectins, suggesting that the reduction in Glc concentration represented a relative increase in the proportion of water-soluble polyuronides at R3 and R4. This is supported by the higher mol % values of Ara and Rha, sugars commonly found in the backbone and side chains of pectins, and the increase in relative abundance of water-soluble UA at these later ripening stages (Table I). The

Table II. *Neutral sugar composition of melon cell wall-polymer fractions*

Fraction	Stage	Rha	Fuc	Ara	Xyl	Man	Gal	Glc
				mol %				
Crude cell wall (AIS)	IG	3.1	2.2	15.3	19.3	8.4	41.5	10.1
	MG	2.9	2.4	14.2	18.2	7.2	39.1	16.0
	R1	2.9	1.8	14.0	19.7	8.0	35.1	18.5
	R2	2.7	2.6	13.9	19.4	6.7	35.1	19.6
	R3	3.7	2.7	12.5	25.8	8.4	31.4	15.6
	R4	3.3	3.3	10.6	29.1	8.6	30.3	14.7
Water-soluble	IG	1.2	1.7	24.0	11.0	5.4	45.1	11.6
	MG	1.0	1.0	18.9	11.5	5.4	50.4	11.8
	R1	1.1	1.0	24.0	15.2	4.6	40.4	13.7
	R2	2.1	1.2	22.0	14.8	3.3	43.3	13.3
	R3	3.3	1.0	26.9	14.5	4.4	39.6	10.2
	R4	3.7	1.0	32.5	15.2	3.3	36.2	8.1
CDTA-soluble	IG	9.2	0.0	27.0	3.8	3.9	46.0	10.2
	MG	10.8	0.0	27.3	4.4	3.7	42.3	11.5
	R1	9.4	1.2	23.2	4.9	3.1	44.6	13.7
	R2	8.0	0.0	23.5	4.9	2.3	43.1	18.2
	R3	9.6	0.0	24.0	7.6	3.0	39.2	16.6
	R4	7.7	2.5	25.8	12.7	4.7	33.8	12.8
Na_2CO_3-soluble	IG	6.0	0.0	21.7	4.2	0.5	67.0	0.6
	MG	5.9	0.5	22.6	4.6	0.7	63.6	2.2
	R1	6.3	0.0	22.2	8.1	0.5	60.1	2.7
	R2	5.5	0.5	20.0	6.1	0.8	63.3	4.0
	R3	4.4	0.0	21.6	6.8	1.0	62.4	3.8
	R4	3.7	0.0	24.1	10.8	2.0	54.3	5.1
4% KOH-soluble	IG	1.1	0.4	5.5	46.1	1.5	24.8	20.7
	MG	1.2	0.7	5.0	36.8	1.8	21.2	33.2
	R1	1.7	1.6	5.5	37.1	2.4	23.5	28.1
	R2	1.8	2.1	6.0	27.4	2.2	25.4	35.2
	R3	0.8	1.2	8.1	28.7	4.4	19.5	37.3
	R4	1.6	1.8	5.9	24.8	2.9	20.3	42.7
24% KOH-soluble	IG	1.4	2.5	6.8	22.2	4.9	26.3	36.0
	MG	0.9	1.7	4.5	23.3	5.6	22.7	41.2
	R1	0.9	1.8	3.3	27.2	4.3	20.3	42.2
	R2	0.9	1.9	2.8	28.8	2.7	17.0	45.9
	R3	1.0	2.1	3.5	33.8	3.3	15.8	40.5
	R4	1.2	2.0	3.0	30.3	4.6	14.4	44.6
Residue	IG	0.0	0.0	0.5	0.3	13.8	4.0	81.4
	MG	0.0	0.0	0.0	0.0	13.4	4.1	82.5
	R1	0.0	0.0	0.0	0.0	12.5	5.0	82.5
	R2	0.0	0.0	0.4	0.6	13.5	3.5	81.9
	R3	0.0	0.0	0.0	0.0	8.8	4.5	86.6
	R4	0.0	0.0	1.6	0.8	7.9	4.1	85.6

proportion of Xyl increased marginally prior to softening, thereafter remaining constant.

A similar distribution of neutral sugars was detected in the CDTA-soluble fraction, with high concentrations of Ara and Gal, which again decreased during ripening, particularly between R3 and R4. Relative to the other pectin-rich fractions, there was a high ratio of Rha to Gal and Ara, possibly indicative of a less substituted rhamnogalacturonan pectic backbone, typical for pectins from the middle lamella (Brett and Waldron, 1996). The proportions of Xyl, Man, and Fuc all increased late in ripening.

A very high mol % of Gal was evident in Na_2CO_3-soluble polymers, which, together with Rha, declined through ripening, whereas the relative concentrations of Xyl, Man, and Glc increased. This coincided with a reduction in the relative amounts of UA (Table I) and indicates a loss of pectins from this fraction at R3 and R4. The relatively high ratio of Gal to Rha suggests a greater degree of substitution of the pectin backbone with Gal-rich side chains.

Taken together, these data suggest that the relative solubility of pectic polysaccharides exhibited no change between IG and R1. The loss of covalently bound pectins between R1 and R2 coincided with an increase in chelator-extractable pectins, whereas increases in water-soluble polyuronides occurred in the last two softening stages, R3 and R4.

Yield and Composition of Hemicellulosic and Residual Fractions

The 4 and 24% KOH and residue fractions together contained only minor quantities of UA (Table I) and these were mostly associated with the cell wall residue (α-cellulose). The greatest proportion of TS was extracted by 24% KOH, and this fraction showed a two-step reduction, declining 10% from MG to R1, followed by a 10% reduction between R2 and R4, although the overall proportion of TS with respect to the AIS showed a decline from MG through ripening. The TS detected in the residue increased from IG to R1, showed a reduction at R2, and remained constant through the overripe stage, although the proportion of TS relative to the TS in the AIS increased until R1 and showed little change through ripening. The 4% KOH-extracted material also showed a transient increase in the concentration of TS, peaking at R1, whereas the proportion of the overall TS remained relatively constant.

In the 4 and 24% KOH-soluble fractions, the principal neutral sugars were Xyl, Gal, and Glc (Table II). The proportion of Xyl was especially high in the 4% KOH-soluble fraction and decreased dramatically during softening (46% reduction from IG to R4), particularly prior to and coincident with the onset of softening. The levels of Glc increased throughout ripening, whereas those of the other sugars remained relatively constant or showed no clear pattern. Conversely, the Gal mol % decreased throughout ripening in the 24% KOH-soluble polymers, and values for Glc showed no apparent trend. The mol % of Xyl and Ara increased and decreased, respectively, from IG through ripening. In the residual cell wall material, Glc represented by far the predominant neutral sugar, almost certainly the result of partial hydrolysis of cellulose by the TFA treatment, with no change in relative abundance during softening. However, high levels of Man were present and declined from R2 to R4, in addition to smaller quantities of Gal, which showed no change in the ripening series.

Gel Chromatography of Pectic Cell Wall Fractions and Compositional Analysis of Subfractions

To examine changes in the molecular mass of the constituent polysaccharides during softening, cell wall fractions were subjected to size-exclusion chromatography. Column fractions were assayed specifically for UA in the pectin-rich fractions and for xyloglucan in the hemicellulose-rich fractions, as well as for TS to assess the presence of additional polysaccharides representing other cell wall components. Following the identification of particular size classes of polymers, indicated by the presence of distinct peaks, subfractions were pooled and their neutral sugar compositions were examined to establish whether particular polysaccharide types could be assigned to specific size fractions.

Water-Soluble Fraction

Size fractionation of water-soluble polymers on a Sepharose CL-4B column (dextran fractionation range of 30–5000 kD) gave a single broad peak of UA with an average molecular mass close to the 260-kD dextran marker (Fig. 3) and a trace amount of UA in the void volume, suggesting that the pectins had been well fractionated. The profile of TS was also within the fractionation range, and at least two additional peaks were detected at approximately 11 kD and in the total volume. Between MG and R1 there was an apparent increase in the molecular size of the polyuronide peak, and an increase in the proportion of high-molecular-mass pectins fractionating at or near the void volume. From R2 to R3, a gradual decrease in molecular mass occurred until the profile of polyuronides at R3 appeared similar to that at IG. However, in the overripe stage (R4) a complete loss of high- and intermediate-molecular-mass pectins was indicated by a single symmetrical peak of polyuronides, corresponding to the 38-kD marker.

Four peaks were identified based on TS and UA assays, and subfractions were pooled for neutral sugar composition analysis (Fig. 3). Subfraction i was comprised of polymers eluting in the void volume and represented only a minor portion of the total polysaccharides in this fraction, showing no change in relative prominence during ripening until R4, when no high-molecular-mass polymer remained. The neutral sugar composition was also similar between IG and R1, comprising mainly Ara (60–70%), with smaller amounts of Glc, Gal, and Man (Table III).

Subfraction ii corresponded to the major peak of the polyuronide and TS profiles from IG, R1, and R4, but comprised lower-molecular-mass polymers at the latter stage following a large decrease in polymer size. A high relative ratio of UA to TS was evident, and neutral sugar analysis revealed a large mol % of Gal, together with Ara and Glc. The concentrations of Glc and Gal were greater at R1 than at IG, and, although this subfraction at R4 also comprised mainly Gal, Ara, and Glc, an increased proportion of Xyl was also detected.

Subfraction iii had a greater ratio of TS to UA and consisted of Glc, Xyl, Man, and Gal. The proportion of Ara increased at R1, coincident with a greater prominence of the peak, whereas the amount of Xyl decreased. By R4, the concentration of Ara had decreased, whereas that of Man had increased.

Subfraction iv represented relatively low-molecular-mass polymers that were comprised mainly of Glc, Gal, and Man. Higher levels of Ara were seen at R1, coincident with a substantial peak increase, whereas the proportion of Xyl increased substantially from 5% at R1 to 43% at R4 as the peak showed a relative decline.

Assignment of subfraction numbers to particular fractions was complicated by shifts in the elution profiles. For example, subfraction ii spanned the peak of polyuronides at IG, the lower-molecular-mass side of the peak at R1, and the higher-molecular-mass polyuronides at R4. Thus, the subfractions may represent the same classes of polysaccharides following changes in molecular mass or they may represent different classes of polymers. However, the neutral sugar composition of subfraction iii at R4 was more similar to that of subfraction iii of R1 than to ii of R1, suggesting that depolymerization of the principal poly-

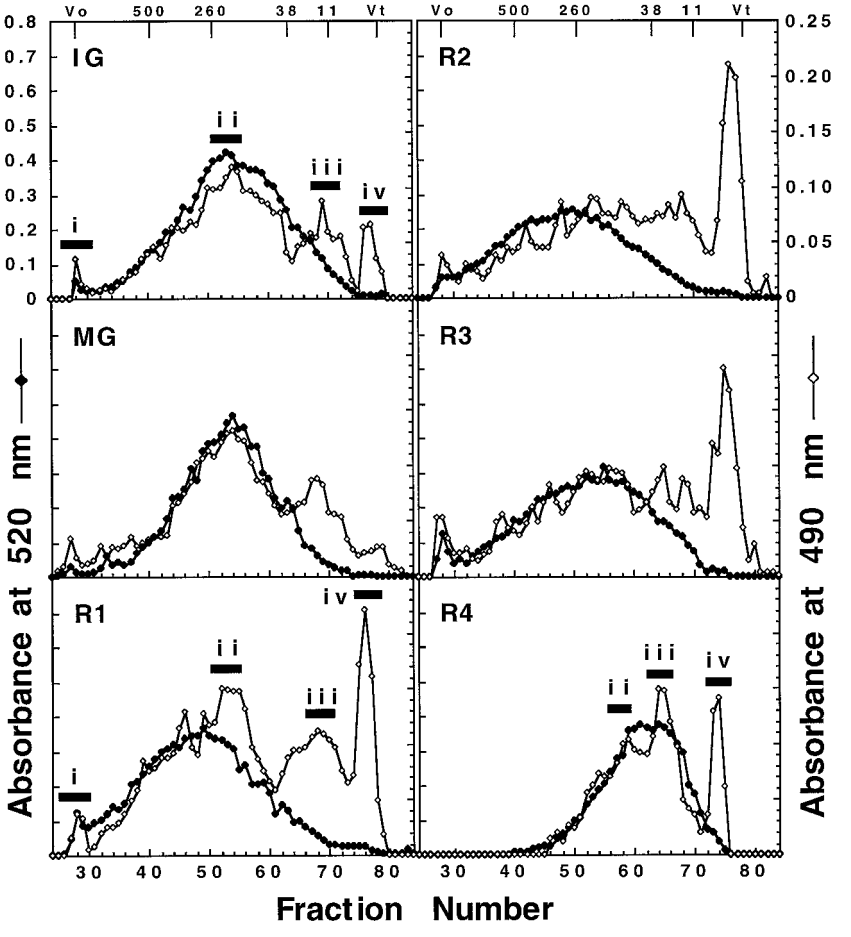

Figure 3. Gel-filtration profiles of water-soluble polysaccharides derived from six developmental stages of Charentais melon fruit fractionated on Sepharose CL-4B. Column fractions (2.0 mL) were assayed for UA content (●) using the *m*-hydroxybiphenyl method (Blumenkrantz and Asboe-Hansen, 1973) or for TS (○) using the phenol-sulfuric acid method (Dubois et al., 1956). Dextran molecular-mass markers (kD) used as a calibration scale are shown at the top. i through iv, Subfractions described in the text; V_o, void volume; V_t, total volume.

mers in subfraction iii was substantially less than that indicated for the polyuronides.

CDTA-Soluble Fraction

This fraction was characterized by a peak of excluded high-molecular-mass pectins, and a broad population of polymers peaking between 260 and 500 kD (Fig. 4). The gel-filtration profile revealed an increase in the relative amount of excluded material until R2, followed by a marked decrease through the later ripening stages. A downshift in the polyuronide profile was seen in the last two stages, resulting in an average molecular mass of approximately 260 kD at R4 and a small proportion of polysaccharide in the void volume. In general, the profiles of TS and polyuronides paralleled each other, with no appearance of additional peaks.

Na_2CO_3-Soluble Fraction

The chromatographic separations of Na_2CO_3-soluble polymers in common with those of the CDTA-solubilized material, resulted in similar profiles when assayed for UA or TS (Fig. 5), although the ratios of UA to TS varied across the fractionation range of the column, suggesting a greater association of neutral sugars with particular molecular-size classes. Four peaks (i, ii, iii, and iv) were identified, corresponding to fractions in the void volume, between the void volume and the 500-kD marker, close to the 260-kD marker, and between the 11- and 38-kD markers, respectively. Subfractions spanning these peaks were pooled for neutral sugar analysis (Table III).

The composition of subfraction i remained relatively consistent throughout the series, comprising primarily Gal and Ara with some additional Rha and Glc, and the profile exhibited no clear pattern of increase or decrease through ripening. Subfraction ii had an especially high ratio of TS relative to UA, and corresponded to large-molecular-size polymers, which showed a decrease in molecular mass between R2 and R4. GC analysis revealed an extremely high proportion of Gal (more than 70 mol %) at IG and R1, whereas by R4 a relative reduction of 20% had occurred. The proportion of Rha increased coincident with the loss of Gal at R4.

The neutral sugar composition and large molecular size are consistent with the profile of subfraction ii, depicting a loss of Gal-rich neutral sugar side chains from rhamnogalacturonan I, a common pectic polymer with a backbone of alternating α-1,4-galacturonosyl and α-1,2-rhamnosyl residues, which has been described in other ripening fruit (Seymour et al., 1990; Redgwell et al., 1992). The elution point of the peak changed only slightly through ripening.

Table III. *Neutral sugar composition of subfractions collected from size-fractionated melon cell wall extracts*

Fraction	Stage	Subfraction	Rha	Fuc	Ara	Xyl	Man	Gal	Glc
						mol %			
Water-soluble	IG	i	0.0	0.0	69.2	0.0	7.7	11.5	11.5
		ii	0.0	0.0	30.6	7.2	0.0	51.2	11.0
		iii	0.0	0.0	7.4	25.6	24.7	12.3	29.9
		iv	0.0	0.0	0.0	6.7	10.6	21.8	60.9
	R1	i	0.0	0.0	61.0	0.0	5.9	15.4	17.7
		ii	0.0	0.0	14.5	0.0	0.0	58.1	27.4
		iii	0.0	0.0	21.4	10.7	23.5	15.4	29.1
		iv	0.0	0.0	13.7	5.1	25.6	18.5	37.0
	R4	i	N/D[a]	N/D	N/D	N/D	N/D	N/D	N/D
		ii	0.7	0.7	15.0	17.2	3.4	39.6	23.5
		iii	0.0	1.7	7.0	14.5	30.8	14.0	32.0
		iv	0.8	0.5	5.9	43.2	5.4	15.2	29.1
Na_2CO_3-soluble	IG	i	9.5	0.0	15.8	2.1	0.0	61.1	11.4
		ii	6.2	0.0	12.2	0.9	0.0	75.7	5.0
		iii	12.8	0.0	17.1	10.3	0.0	55.5	4.3
		iv	14.0	0.0	55.2	10.5	0.0	8.7	11.6
	R1	i	9.1	0.0	23.0	0.0	0.0	56.8	11.1
		ii	6.9	0.0	18.5	1.2	0.0	71.7	1.8
		iii	6.6	0.0	14.1	8.5	0.0	63.5	7.4
		iv	8.0	0.0	17.3	14.3	0.0	49.8	10.6
	R4	i	9.0	0.0	21.7	6.9	0.0	55.7	6.6
		ii	17.6	0.0	12.9	5.4	0.0	60.3	3.8
		iii	2.5	0.0	14.9	16.1	0.0	62.2	4.2
		iv	13.4	0.0	9.2	39.7	0.0	32.1	5.6
4% KOH-soluble	IG	i	4.5	0.0	19.0	8.6	6.1	40.3	21.5
		ii	0.0	0.0	7.0	69.3	5.6	11.3	6.8
		iii	0.0	0.4	8.0	33.6	0.2	21.7	36.1
		iv	0.6	1.0	14.9	57.2	1.2	16.7	8.4
	R1	i	4.5	0.0	15.8	14.8	4.9	40.3	19.7
		ii	0.0	2.8	5.8	34.9	4.3	24.0	28.1
		iii	0.0	2.9	7.0	28.5	3.5	18.2	40.0
		iv	0.0	1.4	11.4	54.7	2.3	17.7	12.5
	R4	i	5.0	0.0	13.6	10.9	9.1	31.8	29.5
		ii	0.0	3.0	4.5	29.9	1.8	20.9	39.8
		iii	0.0	3.3	3.9	33.4	2.8	17.4	39.2
		iv	0.0	1.9	4.2	59.3	1.8	12.8	20.1
24% KOH-soluble	IG	i	0.0	0.0	13.4	26.7	11.1	22.3	26.5
		ii	0.0	0.0	9.8	14.9	0.0	33.0	42.3
		iii	0.0	0.0	0.0	13.9	0.0	48.5	37.7
		iv	0.0	0.0	17.4	22.4	0.0	10.4	49.8
	R1	i	0.0	0.0	26.8	24.1	4.5	17.9	26.8
		ii	0.0	0.7	2.5	19.4	4.6	26.9	46.0
		iii	0.0	0.0	1.2	26.9	3.7	27.4	40.8
		iv	0.0	0.0	4.7	25.2	15.1	26.9	28.2
	R4	i	0.0	0.0	27.2	29.6	0.0	14.4	28.8
		ii	0.0	0.0	3.1	14.0	0.0	27.0	55.9
		iii	0.0	0.0	5.2	23.5	7.0	27.4	37.0
		iv	0.0	0.0	17.9	28.5	25.6	8.4	19.6

[a] N/D, Not detected.

Peak iii had a similar composition to peak ii, comprising primarily Gal and Ara, but with a ratio of TS to UA approximately one-half that of subfraction ii and a greater proportion of Rha, suggesting the presence of less-substituted pectins. High levels of Rha were detected at IG and declined in later stages, coincident with an increase in the mol % concentrations of Gal and Xyl and the decreased relative prominence of the peak.

Subfraction iv comprised lower-molecular-mass polymers and at IG, exhibited a low ratio of TS to UA and a high proportion of Rha and Ara (14 and 55 mol %, respectively). By R1 the ratio had increased, as had the relative amount of

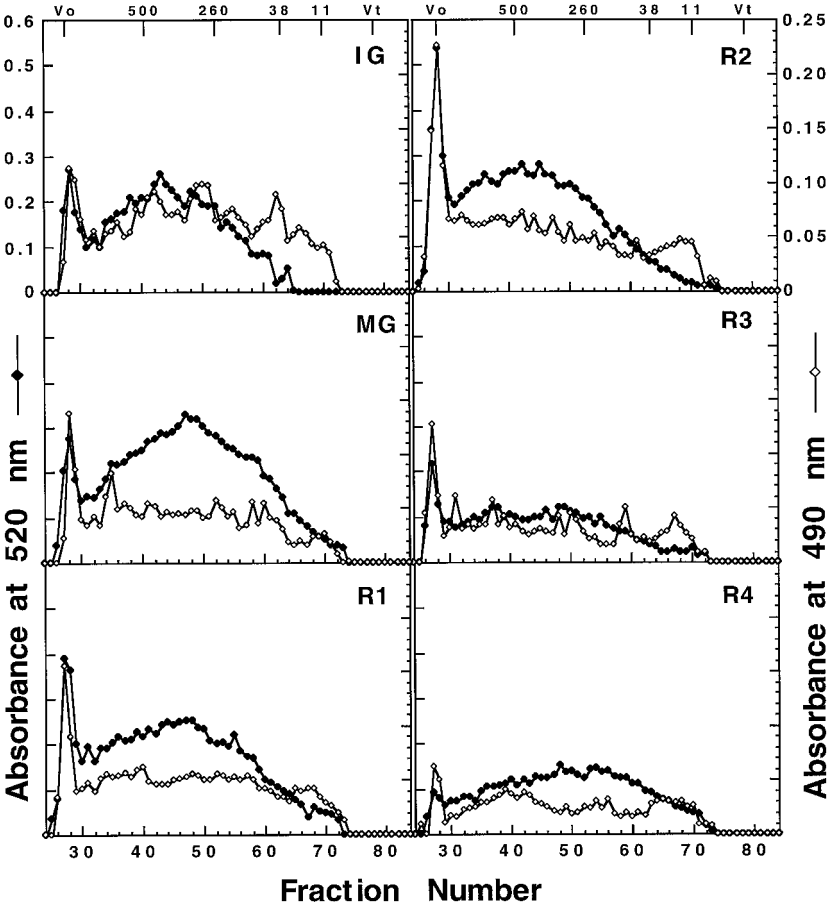

Figure 4. Gel-filtration profiles of CDTA-soluble polysaccharides derived from six developmental stages of Charentais melon fruit. Details are as described for Figure 3.

Gal (approximately 9–50 mol %), although Ara decreased to a similar degree, suggesting that depolymerization of higher-molecular-mass Gal-rich polymers contributed to this subfraction. The relative size and profile of peak iv changed little during softening, although the proportions of Xyl and Ara increased and decreased, respectively. The high level of Xyl in this subfraction (Table III) and in the CDTA-extracted polymers (Table II), especially at R4, has previously been reported in other fruit (Seymour et al., 1990; Martin-Cabrejas et al., 1994), where it was suggested to originate from xylans and proposed to reflect the existence of xylan-pectin complexes (Martin-Cabrejas et al., 1994). In general, the size distribution of Na_2CO_3-extracted polymers showed a relative downshift only in the last ripening stage.

During ripening the pectin concentration of the cell wall (AIS) remained relatively constant, showing an approximately 10% decrease between the pre- and overripe stages. However, there was clear evidence of pectin solubilization and depolymerization during softening. At the onset of softening, substantial solubilization of polyuronides from the Na_2CO_3-soluble fraction coincided with an increase in chelator-soluble pectins, suggesting that once released from the wall, a proportion of the covalently bound pectins became ionically associated. Subsequently, at the R3 stage, continued losses from the Na_2CO_3-soluble fraction corresponded to large increases in polyuronides and TS in the water-soluble fraction that continued until R4. This, in addition to the neutral sugar composition of the fractions, suggests solubilization of covalently bound pectins into the water-soluble fraction, as has been reported in tomato (Carrington et al., 1993). At R4 the water-solubilized pectins underwent a dramatic downshift in molecular mass. Depolymerization of pectins in the Na_2CO_3- and CDTA-soluble fractions was more modest, but also occurred primarily late in ripening.

The exact mechanisms underlying such pectin metabolism during ripening remain unclear and may reflect the cumulative effects of both enzymatic and nonenzymatic processes. In many fruits, including tomato, pectin degradation has been associated with the action of *endo*-PG. However, in melon a decrease in the molecular mass of polyuronides has previously been reported to occur in the apparent absence of PG activity (McCollum et al., 1989), and other melon cultivars are described as lacking PG activity. In an accompanying paper (Hadfield et al., 1998), we report the identification of a Charentais melon PG gene family and describe the expression of three PG mRNAs, primarily in the later stages of ripening fruit. This suggests that PG may participate in pectin metabolism in melon, particularly in pectin depolymerization evident in the late stages of fruit softening. However, solubilization of covalently associated pectins was apparent prior to the detection of PG mRNAs, suggesting that PG-independent as

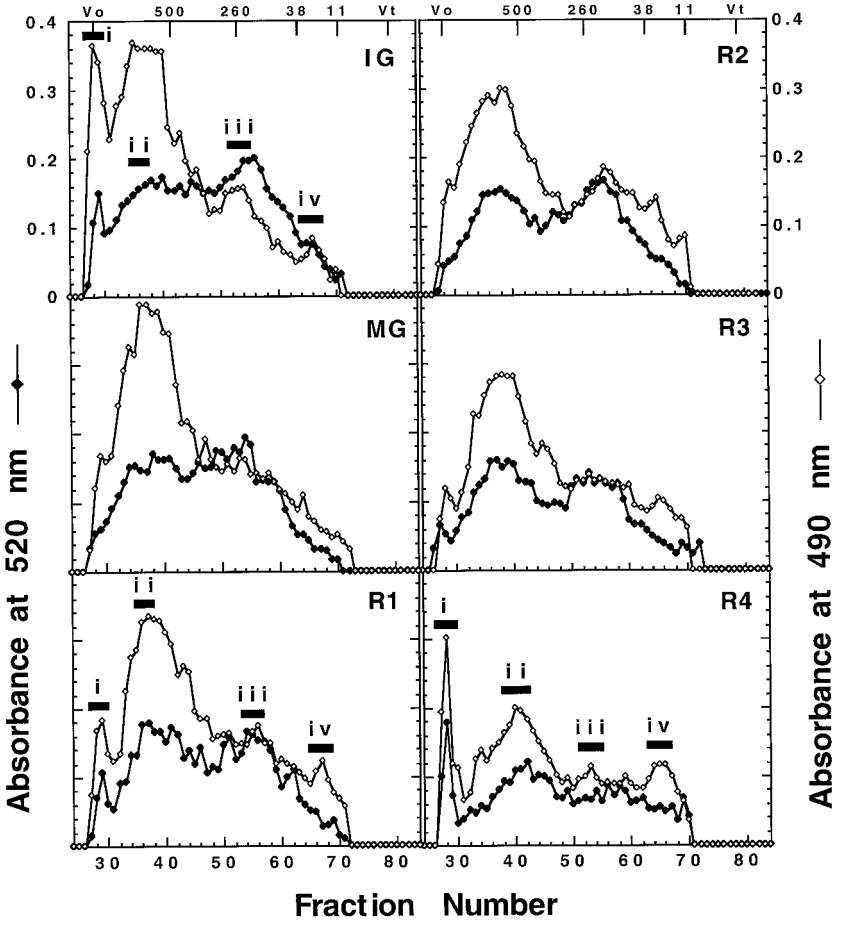

Figure 5. Gel-filtration profiles of Na_2CO_3-soluble polysaccharides derived from six developmental stages of Charentais melon fruit. Details are as described for Figure 3.

well as PG-dependent processes may contribute to overall pectin disassembly.

It has been suggested that pectin solubilization may result from the loss of galactosyl residues in the form of the neutral Gal-rich side chains of rhamnogalacturonans (Seymour et al., 1990; Redgwell et al., 1992). Such degalactosylation is typically seen in ripening fruit, and although the structural relevance has not been demonstrated, galactans may be integral to the formation of a cohesive pectin matrix, cross-linking pectin molecules with each other, as well as with hemicelluloses and other cell wall components.

The loss of Gal can occur independently of PG activity (Carrington et al., 1993), suggesting the involvement of other classes of enzymes such as β-galactosidases/β-galactanases, which have been associated with many ripening fruits (Ross et al., 1993, 1994; Carey et al., 1995; Lashbrook et al., 1997), and which may act on several classes of polysaccharides, including the galactan side chains of rhamnoglacturonans (Pressey, 1983). Loss of galactans has been demonstrated to accompany or even precede increased solublization of polyuronides (Gross and Wallner, 1979; Kim et al., 1991), and purified or partially purified β-galactosidase has been shown to catalyze an apparent decrease in the molecular size of pectins in vitro in tomato (De Veau, 1993) and melon fruits (Ranwala et al., 1992).

Gel Chromatography of Hemicellulosic Cell Wall Fractions and Compositional Analysis of Subfractions

4% KOH-Soluble Fraction

Hemicellulosic material was size-fractionated on a Sepharose CL-6B column (dextran fractionation range of 10–1000 kD), and fractions were assayed for xyloglucan and TS. Size separation of 4% KOH-soluble polymers (Fig. 6) revealed a large peak of excluded polysaccharides (subfraction i) that showed a relative decline from R2 to R4. Compositional analysis indicated that at the IG and R1 stages, prior to its loss, subfraction i was particularly rich in Gal (40 mol %), with smaller amounts of Ara and Glc (Table III) and approximately 5 mol % Rha. The presence of substantial amounts of Gal and Ara in discrete, high-molecular-mass hemicellulosic polymers (> 1000 kD) has been described previously (Talbott and Ray, 1992). This was attributed to the presence of large arabinogalactan molecules, possibly comprised of glycosidically linked arabinan and galactan subunits.

Arabinogalactans or arabinans and galactans have been identified as side chains of rhamnogalacturonans or proposed to exist as free macromolecules, possibly forming a separate layer surrounding the xyloglucan/cellulose network (Talbott and Ray, 1992). A prominent peak of xylo-

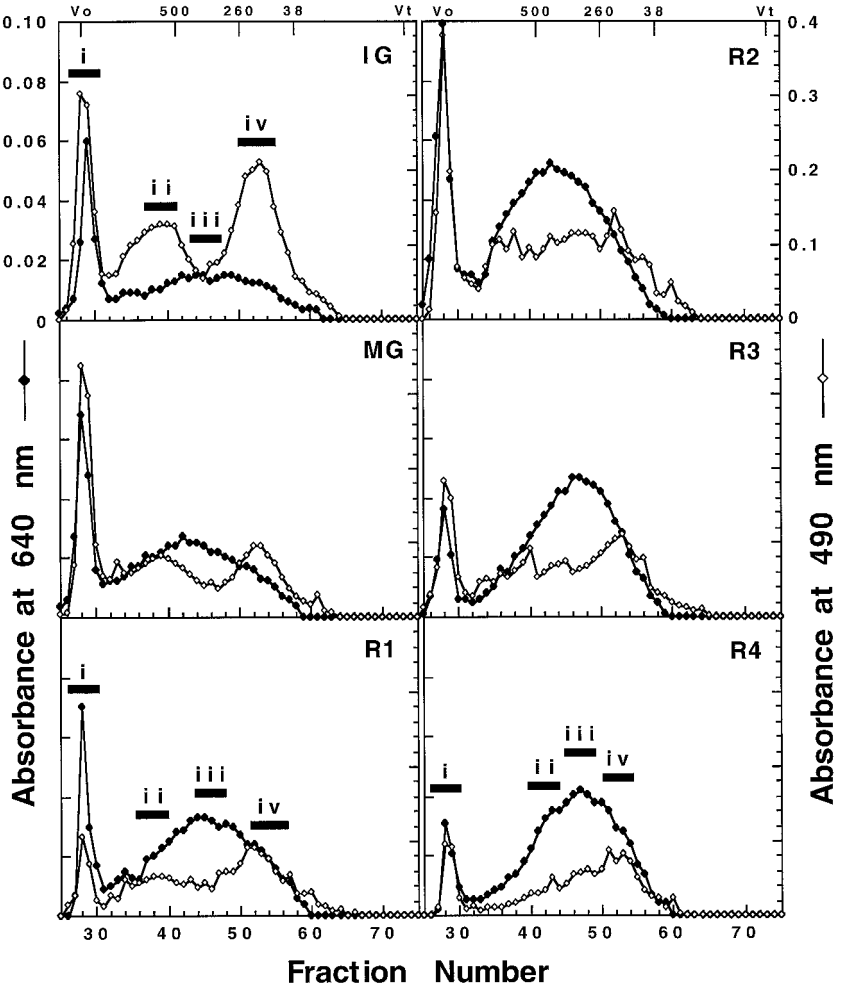

Figure 6. Gel-filtration profiles of 4% KOH-soluble polysaccharides derived from six developmental stages of Charentais melon fruit and fractionated on Sepharose CL-6B. Column fractions (2.0 mL) were assayed for xyloglucan (●) as described in Maclachlan and Brady (1994) or for TS (○) using the phenol-sulfuric acid method (Dubois et al., 1956). Details are as described for Figure 3.

glucan co-eluted in the void volume and showed a similar pattern during softening to that of the arabinogalactan-rich TS peak, exhibiting apparent degradation in the last two ripening stages. Relatively few reports exist of similarly extracted and fractionated hemicellulosic polymers from fruit, since the hemicellulose fraction is typically isolated using much higher concentrations of alkali in a single step, rather than in two steps with an initial lower concentration as described here.

Cutillas-Iturralde et al. (1994) assayed a similar wall fraction, extracted with 0.5 M KOH from ripening persimmon, for xyloglucan and TS and described an excluded peak of TS. However, this peak was not coincident with appreciable quantities of xyloglucan, which generally fractionates within the column range. Hemicelluloses extracted from vegetative tissues with low concentrations of alkali and size-fractionated have been reported to exhibit a similar pattern (Nishitani and Masuda, 1983; Lorences and Zarra, 1987; Lorences et al., 1987); xyloglucan and a population of high-molecular-mass polymers assayed for TS, often rich in Ara and Gal, are resolved as discrete peaks or with excluded xyloglucan representing a minor component of the total xyloglucan in that fraction. Figure 6 shows that the xyloglucan in the void volume comprised an atypically large proportion of the total xyloglucan in this fraction, but that the ratio of excluded to included xyloglucan decreased dramatically at R3 and R4. At R4, in addition to a reduction in the relative size of the peak, the proportion of Gal had decreased 10 mol %, whereas Glc showed an equivalent increase.

Earlier models of the primary cell wall proposed a covalently linked macromolecule of noncellulosic polysaccharides: xyloglucan to arabinogalactans, arabinogalactans to pectins, and pectins to structural cell wall proteins. (Keegstra et al., 1973). More recently, the idea of predominantly noncovalent associations between matrix polymers has received attention (Varner and Lin, 1989; Talbott and Ray, 1992; Carpita and Gibeaut, 1993). It has been pointed out that almost all of the polyuronide component of the cell wall can be chemically extracted under relatively mild conditions, without the concomitant release of xyloglucan, arabinogalactan, or other hemicelluloses (Talbott and Ray, 1992). However, the possibility of covalent bonds between a small subset of the pectin, arabinogalactan, and xyloglucan populations should not be excluded. The coelution of an unusually high-molecular-mass xyloglucan with a Gal- and Ara-rich polymer and a small amount of Rha following a chemical extraction expected to disrupt alkali-labile link-

ages might suggest a covalent association between large arabinogalactan polymers and xyloglucan. The formation of such a complex could prevent a portion of the xyloglucan from chromatographing within the column range, as is apparent in Figure 6.

A second broad peak of xyloglucan with an average molecular mass of between 260 and 500 kD showed a large increase in abundance from IG to R2, where a slight upshift was detected, followed by depolymerization at R3 and R4. The neutral sugars in subfraction iii at the peak of this xyloglucan profile were comprised of mainly Glc, Gal, and Xyl (Table III), typical components of xyloglucan. The proportions of neutral sugars were similar to those reported for weak-alkali-solubilized xyloglucan from bean (Nishitani and Masuda, 1983), and the detectable levels of Fuc suggest that the xyloglucan in this peak was fucosylated. The ratio of sugars showed little variation during softening.

The TS profile at IG indicated the existence of two unique and substantial populations of polysaccharides (Fig. 6, ii and iv) that did not correspond to the xyloglucan profile. Both peaks declined dramatically between IG and MG and were largely indistinguishable in the later ripening stages. Analysis of the neutral sugar composition of ii (Table III) showed a high proportion of Xyl, which fell from 70 to 35 mol % between IG and R1, coincident with an increase in the proportion of Glc, Gal, and Fuc, suggesting the loss of a Xyl-rich polymer and a relative increase in the proportion of xyloglucan in this fraction prior to ripening. Subfraction iv was also rich in Xyl, although the mol % did not change to a great extent during ripening. Glc and Fuc increased between IG and R1, coincident with a slight decrease in Ara and Xyl and a decline in the overall prominence of the peak, suggesting an increase in the proportion of xyloglucan and a relative decrease in xylans. A small amount of UA was detected in this subfraction (data not shown), suggesting the presence of xylans, glucuronoxylans, and/or glucuronoarabinoxylans.

Putative xylan-pectin complexes in ripening tomato fruit (Seymour et al., 1990) and covalent associations between glucuronoxylans and xyloglucan in olive pulp (Coimbra et al., 1995) have been described, although little has been reported to suggest a role for xylan metabolism in cell wall disassembly during fruit ripening.

24% KOH-Soluble Fraction

The polymers in this fraction mostly eluted as a symmetrical population within the fractionation range of the gel, with a single broad peak of xyloglucan near the 500-kD dextran marker (Fig. 7). The profile of TS paralleled that of xyloglucan, however, additional peaks were detected in the void volume and near the 38-kD marker. The ratio of TS to

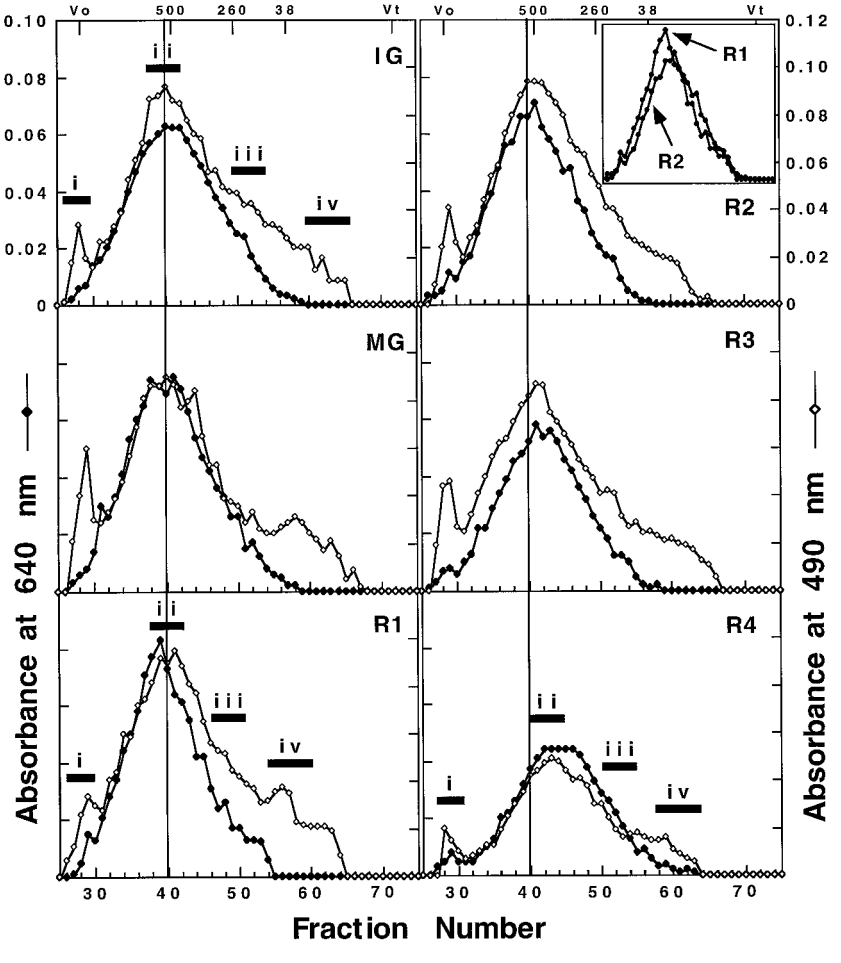

Figure 7. Gel-filtration profiles of 24% KOH-soluble polysaccharides derived from six developmental stages of Charentais melon fruit. The superimposed profiles from the xyloglucan assay of R1 and R2 polymers are shown in the inset, top right. Details are as described for Figures 3 and 6.

xyloglucan was greater in fractions corresponding to lower-molecular-mass xyloglucans (below the 500-kD marker). Subfractions ii and iii consisted almost entirely of Xyl, Gal, and Glc and trace amounts of Ara and Man (Table III), suggesting a relatively pure xyloglucan fractionation. However, Fuc was not present at detectable levels, suggesting an absence or a much lower degree of fucosylation of this tightly bound xyloglucan population compared with the more readily extracted (4% KOH) xyloglucan.

A slight upshift in elution profile was seen between IG and R1, followed by depolymerization of the entire spectrum of xyloglucan polymers at the onset of softening between R1 and R2, which continued throughout ripening. A similar size distribution of xyloglucan was seen in hemicellulosic extracts from tomato pericarp and locule tissue, and depolymerization was evident during ripening (Maclachlan and Brady, 1994). Comparisons of these data with other fruit and melon varieties is difficult, because the equivalent of 4 and 24% KOH-soluble polymers are typically not considered separately and are co-chromatographed. Figure 7 demonstrates that the depolymerization of tightly bound xyloglucan was coincident with the early onset of softening.

Subfraction i consisted primarily of Glc, Gal, and Xyl (Table III), with a relatively high proportion of Ara (13 mol %) and Man (11 mol %) at IG. UA was also primarily localized in this fraction (data not shown). Apart from a slight decline at R4, the relative prominence of the peak showed little change; however, there was an increase in the relative abundance of Ara between IG and R1. Furthermore, it appeared that a tightly bound, high-molecular-mass, Man-rich polymer or polymer complex underwent depolymerization during ripening, since Man was detected only in subfraction i at IG, showed distribution throughout all the subfractions at R1, and was detected mostly in subfraction iv at R4, where it comprised 26 mol % of the neutral sugars (Table III).

The overall proportion of Man in the AIS did not decrease during ripening (Table II). It is likely that Man was a component of glucomannans and/or galactoglucomannans such as those detected in the 4 M KOH hemicellulose fraction of tomato (Seymour et al., 1990) and pineapple (Smith and Harris, 1995) fruit. It has been suggested that glucomannans and/or galactoglucomannans are not degraded during ripening in tomato (Sakurai and Nevins, 1993); however, continued glucomannan synthesis during tomato fruit ripening has been reported (Tong and Gross, 1988), and analysis of cell wall biosynthesis during tomato ripening also indicated increased incorporation of Xyl and Man residues into hemicellulosic polymers during ripening (Greve and Labavitch, 1991). Therefore, it is possible that the apparent depolymerization of glucomannans in the 24% KOH-soluble material during ripening (Table III) actually reflects solubilization of high-molecular-mass, Man-containing polysaccharides followed by de novo synthesis of lower-molecular-mass glucomannans. Alternatively, since the Man content of the residue fraction showed a major decrease between R2 and R3, a population of lower-molecular-mass glucomannans may be more readily extracted by 24% KOH in the later two ripening stages, R3 and R4.

CONCLUSIONS

A summary of cell wall changes and potential enzyme activities during Charentais melon fruit ripening is shown in Figure 8. Pectinase activity is interpreted to result from the cumulative action of a range of pectolytic enzymes, including those targeting side-chain and backbone linkages of complex pectin molecules. In Charentais melon PG mRNAs were abundant at R2, whereas a peak of pectinase activity was apparent at R3 (see accompanying paper, Hadfield et al., 1998), suggesting that this later peak was the result of PG activity. Studies in tomato also suggest a substantial time lag between the appearance of PG mRNA and either protein or enzyme activity (Brady et al., 1982, 1985; Tucker and Grierson, 1982; Speirs et al., 1989).

Previous reports have associated disassembly of the pectin macromolecular matrix with loss of wall galactans, probably through the action of β-galactosidases/β-galactanases (De Veau et al., 1993; Carey et al., 1995; Lazan et al., 1995). Our data suggest that early loss of Gal coincided temporally with an early peak of pectinase activity in IG fruit, which showed a gradual decline through R2 and may reflect the presence of β-galactosidase/β-galactanase activity. In addition to the loss of Gal from pectic polymers, covalently bound pectins appear to undergo solubilization prior to or coincident with the appearance of PG mRNAs.

A model of pectin disassembly in Charentais melon can therefore be proposed in which loss of Gal, possibly from pectin-associated galactan side chains, contributes to early PG-independent solubilization of covalently linked pectins prior to or coincident with the onset of significant fruit softening. Solubilized pectins are subsequently subject to deglycosylation and depolymerization in the later stages of ripening through the action of *endo-* and/or *exo*-acting PG. The decreases in the molecular mass of polyuronides in all of the pectic fractions in the later stages of ripening also suggest the action of *endo*-PG.

The model summarizes the data obtained from the above experiments and could be expanded to include other enzymic activities that have been associated with pectin metabolism during ripening, such as pectin methylesterase (Tucker et al., 1982; Harriman et al., 1991; Tieman et al., 1992). A similar model of pectin degradation involving the solubilization of the bulk of pectic polymers independent of both PG and β-galactosidase, which act to degrade the solubilized pectins later in softening, has been used to describe cell wall changes in ripening kiwifruit (Redgwell et al., 1992).

Hemicelluloses also show substantial changes in the degree of solubility and molecular mass profiles during ripening. Xyl-rich polymers show substantial degradation prior to ripening (Fig. 8), and it is possible that this is related to the coincident solubilization of pectin-associated Gal, suggesting the existence of xylan-pectin complexes. Of particular interest was a decrease in the molecular mass of the tightly bound xyloglucan fraction coincident with the onset of softening (Figs. 7 and 8). This component of the

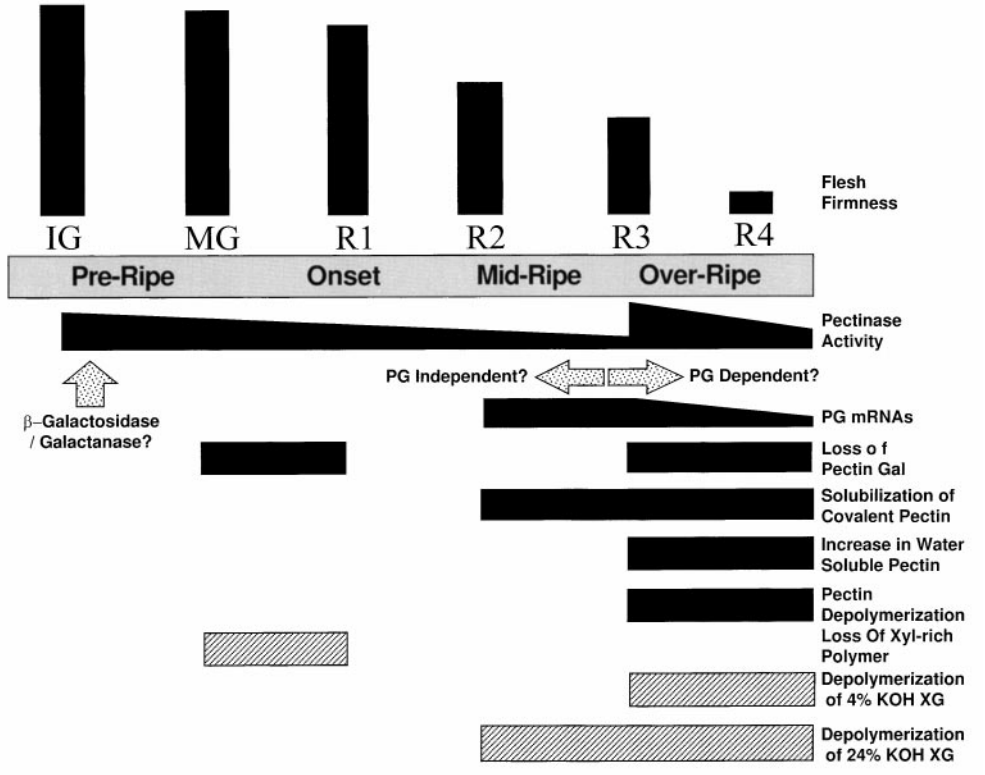

Figure 8. Model of the temporal sequence of cell wall changes, pectinase activity, and PG mRNA expression in ripening Charentais melon fruit at defined developmental stages. XG, Xyloglucan.

wall is presumed to coat and cross-link the cellulose microfibrils, and thus may play an important structural role. Disruption of this close association by cleavage of the xyloglucan cross-links, perhaps catalyzed by endo-1,4-β-glucanases or xyloglucan endotransglycosylases, both of which have been associated with ripening (Lashbrook et al., 1997), could allow cell wall loosening.

Alternatively, disruption of the noncovalent associations between the xyloglucan sheath and the cellulose microfibril could also result in textural changes, as well as an increase in the accessibility of the substrate for enzymic attack by cell wall hydrolases. Expansins are proteins that are thought to disrupt the noncovalent association between cellulose and matrix polysaccharides and could act to regulate noncovalent cell wall polymer associations in ripening fruit. Rose et al. (1997) recently identified and characterized a highly abundant, fruit-ripening-specific expansin gene from tomato, as well as homologs from strawberry and melon. The role of expansins in fruit softening is not clear and is currently under investigation. However, it is possible that they act at the cellulose/xyloglucan interface at the onset of fruit softening, disrupting a crucial structural component of the wall. A consequence of this activity might also be to increase the extent of wall swelling, allowing increased access of other cell wall-degradative enzymes to their substrates and reducing the degree of physical entanglement of cell wall polymers, as has been suggested to occur in ripening kiwifruit (Redgwell et al., 1992; Redgwell and Fry, 1993).

Charentais melons show evidence of modification of both pectic and hemicellulosic polymers during ripening, as do many other fruit species. However, the exceptionally rapid softening allowed a clear delineation of cell wall-disassembly events associated with the early or later stages of ripening that had not been apparent in fruit that undergo more gradual and subtle textural changes. This analysis has suggested that modification of tightly bound hemicellulose, specifically xyloglucan, may represent one of the early changes to the cell wall at the onset of ripening. Research is now in progress, in part through the use of transgenic plants, to determine whether genes associated with hemicellulose metabolism, such as expansins, endo-1,4-β-glucanases, and xyloglucan endotransglycosylases may play an important and perhaps synergistic role in regulating early events in fruit softening.

ACKNOWLEDGMENT

The authors would like to thank Dr. L. Carl Greve for useful discussion and assistance.

Received July 2, 1997; accepted January 8, 1998.

LITERATURE CITED

Ahmed AER, Labavitch JM (1977) A simplified method for accurate determination of cell wall uronide content. J Food Biochem **1:** 361–365

Blakeney AB, Harris PJ, Henry RJH, Stone BA (1983) A simple and rapid preparation of alditol acetates for monosaccharide analysis. Carbohydr Res **11:** 3291–3299

Blumenkrantz N, Asboe-Hansen G (1973) New method for quantitative determination of uronic acids. Anal Biochem **54:** 484–489

Brady CJ (1987) Fruit ripening. Annu Rev Plant Physiol **38:** 155–178

Brady CJ, Macalpine G, McGlasson WB, Ueda Y (1982) Polygalacturonase in tomato fruits and the induction of ripening. Aust J Plant Physiol **9:** 171–178

Brady CJ, McGlasson WB, Pearson JA, Meldrum SK, Kopeliovitch E (1985) Interaction between the amount and molecular forms of polygalacturonase, calcium and firmness in tomato fruit. J Am Soc Hortic Sci **110:** 254–258

Brett CT, Waldron KW (1996) Physiology and Biochemistry of Plant Cell Walls. Chapman and Hall, London

Carey AT, Holt K, Picard C, Wilde R, Tucker GA, Bird CR, Schuch W, Seymour GB (1995) Tomato exo-(1–4)-β-D-galactanase. Plant Physiol **108:** 1099–1107

Carpita NC, Gibeaut DM (1993) Structural models of primary cell walls in flowering plants: consistency of molecular structure with the physical properties of the walls during growth. Plant J **3:** 1–30

Carrington CMS, Greve CL, Labavitch JM (1993) Cell wall metabolism in ripening fruit. Plant Physiol **103:** 429–434

Coimbra MA, Rigby NM, Selvendran RR, Waldron KW (1995) Investigation of the occurrence of xylan-xyloglucan complexes in the cell walls of olive pulp (*Olea europaea*). Carbohydr Polym **27:** 277–284

Crookes PR, Grierson D (1983) Ultrastructure of tomato fruit ripening and the role of polygalacturonase isoenzymes in cell wall degradation. Plant Physiol **72:** 1088–1093

Cutillas-Iturralde A, Zarra I, Fry SC, Lorences EP (1994) Implication of persimmon fruit hemicellulose metabolism in the softening process: importance of xyloglucan endotransglycosylase. Physiol Plant **91:** 169–174

Cutillas-Iturralde A, Zarra I, Lorences EP (1993) Metabolism of cell wall polysaccharides from persimmon fruit: pectin solubilization during fruit ripening occurs in the apparent absence of polygalacturonase activity. Physiol Plant **89:** 369–375

De Veau EJI (1993) Degradation and solubilization of pectin by β-galactosidases purified from avocado mesocarp. Physiol Plant **87:** 279–285

Dubois M, Gilles KA, Hamilton JK, Rebers PA, Smith F (1956) Colorimetric method for determination of sugars and related substances. Anal Chem **28:** 350–356

Fischer RL, Bennett AB (1991) Role of wall hydrolases in fruit ripening. Annu Rev Plant Physiol Plant Mol Biol **42:** 675–703

Giovannoni JJ, DellaPenna D, Bennett AB, Fischer RL (1989) Expression of a chimeric polygalacturonase gene in transgenic *rin* (ripening inhibitor) tomato fruit results in polyuronide degradation but not fruit softening. Plant Cell **1:** 53–63

Greve LC, Labavitch JM (1991) Cell wall metabolism in ripening fruit. Plant Physiol **97:** 1456–1461

Gross KC, Sams CE (1984) Changes in cell wall neutral sugar composition during fruit ripening: a species survey. Phytochemistry **23:** 2457–2461

Gross KC, Wallner SJ (1979) Degradation of cell wall polysaccharides during tomato fruit ripening. Plant Physiol **63:** 117–120

Hadfield KA, Rose JKC, Bennett AB (1995) The respiratory climacteric is present in Charentais (*Cucumis melo* cv. Reticulatus F1 Alpha) melons ripened on or off the plant. J Exp Bot **46:** 1923–1925

Hadfield KA, Rose JKC, Bennett AB (1998) Polygalacturonase gene expression in ripe melon fruits supports a role for polygalacturonase in ripening-associated pectin disassembly. Plant Physiol **117:** 363–373

Harriman RW, Tieman DM, Handa AK (1991) Molecular cloning of tomato pectin methylesterase gene and its expression in Rutgers, ripening inhibitor, nonripening and never ripe tomato fruits. Plant Physiol **97:** 80–87

Hayashi T, Maclachlan G (1984) Pea xyloglucan and cellulose I. Macromolecular organization. Plant Physiol **75:** 596–604

Hobson G, Grierson D (1993) Tomato. *In* G Seymour, J Taylor, G Tucker, eds, Biochemistry of Fruit Ripening. Chapman and Hall, London, pp 405–442

Huber DJ (1983) The role of cell wall hydrolases in fruit softening. Hortic Rev **5:** 169–215

Huber DJ (1992) The inactivation of pectin depolymerase associated with isolated tomato fruit cell wall: implications for the analysis of pectin solubility and molecular weight. Physiol Plant **86:** 25–32

Huber DJ, O'Donoghue EM (1993) Polyuronides in avocado (*Persea americana*) and tomato (*Lycopersicon esculentum*) fruits exhibit markedly different patterns of molecular weight downshifts during ripening. Plant Physiol **102:** 473–480

Keegstra K, Talmadge KW, Bauer WD, Albersheim P (1973) Structure of plant cell walls. III. A model of the walls of suspension-cultured sycamore cells based on the interconnections of the macromolecular components. Plant Physiol **51:** 188–197

Kim J, Gross KC, Solomos T (1991) Galactose metabolism and ethylene production during development and ripening of tomato fruit. Post Biol Tech **1:** 67–80

Kojima K, Sakurai N, Kuraishi S (1994) Fruit softening in banana: correlation among stress-relaxation parameters, cell wall components and starch during ripening. Physiol Plant **90:** 772–778

Kramer M, Sanders RA, Sheehy RE, Melis M, Kuehn M, Hiatt WR (1990) Field evaluation of tomatoes with reduced polygalacturonase by antisense RNA. *In* AB Bennett, S O'Neill, eds, Horticultural Biotechnology. Alan R. Liss, New York, pp 347–355

Lashbrook CC, Brummell DA, Rose JKC, Bennett AB (1997) Non-pectolytic cell wall metabolism during fruit ripening. *In* JJ Giovannoni, ed, Fruit Ripening Molecular Biology. Harwood Academic, Reading, UK (in press)

Lazan H, Selamat MK, Ali ZM (1995) β-Galactosidase, polygalacturonase and pectinesterase in differential softening and cell wall modification during papaya fruit ripening. Physiol Plant **95:** 106–112

Lester GE, Dunlap JR (1985) Physiological changes during development and ripening of "Perlita" muskmelon fruits. Sci Hortic **26:** 323–331

Lorences EP, Suarez L, Zarra I (1987) Hypocotyl growth of *Pinus pinaster* seedlings: changes in the molecular weight distribution of hemicellulosic polysaccharides. Physiol Plant **69:** 466–471

Lorences EP, Zarra I (1987) Auxin-induced growth in hypocotyl segments of *Pinus pinaster* Aiton: changes in molecular weight distribution of hemicellulosic polysaccharides. J Exp Bot **38:** 960–967

Maclachlan G, Brady C (1994) Endo-1,4-β-glucanase, xyloglucanase and xyloglucan endo-transglycosylase activities versus potential substrates in ripening tomatoes. Plant Physiol **105:** 965–974

Martin-Cabrejas M, Waldron KW, Selvendran RR (1994) Cell wall changes in Spanish pear during ripening. J Plant Physiol **144:** 541–548

McCann MC, Wells B, Roberts K (1990) Direct visualization of cross-links in the primary cell wall. J Cell Sci **96:** 323–334

McCollum TG, Huber DJ, Cantliffe DJ (1989) Modifications of polyuronides and hemicelluloses during muskmelon fruit softening. Physiol Plant **76:** 303–308

Mitcham EJ, Gross KC, Ng TJ (1991) Ripening and cell wall synthesis in normal and mutant tomato fruit. Phytochemistry **30:** 1777–1780

Mort AJ, Moerschbacher BM, Pierce ML, Maness NO (1991) Problems encountered during the extraction, purification and chromatography of pectic fragments, and some solutions to them. Carbohydr Res **215:** 219–227

Ng TJ, Tigchelaar EC (1977) Action of the non-ripening fruit (*nor*) mutant on fruit ripening of tomato. J Am Soc Hortic Sci **102:** 504–509

Nishitani K, Masuda Y (1983) Auxin-induced changes in the cell wall xyloglucans: effects of auxin on the two different subfractions of xyloglucans in the epicotyl cell wall of *Vigna angularis*. Plant Cell Physiol **24:** 345–355

Pratt HK (1971) Melons. *In* AC Hulme, ed, Biochemistry of Fruits and Their Products. Academic Press, London, pp 207–233

Pressey R (1983) β-Galactosidases in ripening tomatoes. Plant Physiol **71:** 132–135

Ranwala AP, Suematsu C, Masuda H (1992) The role of β-galactosidases in the modification of cell wall components during muskmelon fruit ripening. Plant Physiol **100:** 1318–1325

Redgwell RJ, Fry SC (1993) Xyloglucan endotransglycosylase activity increases during kiwifruit (*Actinidia deliciosa*) ripening. Plant Physiol **103:** 1399–1406

Redgwell RJ, Melton LD, Brasch DJ (1992) Cell wall dissolution in ripening kiwifruit (*Actinidia deliciosa*). Plant Physiol **98:** 71–81

Rose JKC, Lee HH, Bennett AB (1997) Expression of a divergent expansin gene is fruit-specific and ripening-regulated. Proc Natl Acad Sci USA **94:** 5955–5960

Ross GS, Redgwell RJ, MacRae EA (1993) Kiwifruit beta-galactosidase-isolation and activity against specific fruit cell wall polysaccharides. Planta **109:** 499–506

Ross GS, Wegrzyn T, MacRae EA, Redgwell RJ (1994) Apple β-galactosidase. Plant Physiol **106:** 521–528

Sakurai N, Nevins DJ (1993) Changes in physical properties and cell wall polysaccharides of tomato (*Lycopersicon esculentum*) pericarp tissues. Physiol Plant **89:** 681–686

Schuch W, Kanczler J, Hobson G, Tucker G, Grierson D, Bright S, Bird CR (1991) Fruit quality characteristics of transgenic tomato fruit with altered polygalacturonase activity. Hortscience **26:** 1517–1520

Seymour GB, Colquhoun IJ, Dupont MS, Parsley KR, Selvendran RR (1990) Composition and structural features of cell wall polysaccharides from tomato fruits. Phytochemistry **29:** 725–731

Simandjuntak V, Barrett DM, Wrolstad RE (1996) Cultivar and maturity effects on muskmelon (*Cucumis melo*) colour, texture and cell wall polysaccharide composition. J Sci Food Agric **71:** 282–290

Smith BG, Harris PJ (1995) Polysaccharide composition of unlignified cell walls of pineapple (*Ananas comosus* [L.] Merr.) fruit. Plant Physiol **107:** 1399–1409

Smith CJS, Watson CF, Ray J, Bird CR, Morris PC, Schuch W, Grierson D (1988) Antisense RNA inhibition of polygalacturonase gene expression in transgenic tomatoes. Nature **334:** 724–726

Speirs J, Lee E, Brady CJ, Robertson J, McGlasson WB (1989) Endopolygalacturonase: messenger RNA, enzyme and softening in the ripening fruit of a range of tomato genotypes. J Plant Physiol **135:** 576–582

Talbott LD, Ray PM (1992) Molecular size and separability features of pea cell wall polysaccharides. Plant Physiol **98:** 357–368

Tieman DM, Harriman RW, Ramamohan G, Handa AK (1992) An antisense pectin methylesterase gene alters pectin chemistry and soluble solids in tomato fruit. Plant Cell **4:** 667–679

Tong CBS, Gross KC (1988) Glycosyl-linkage composition of tomato fruit cell wall hemicellulosic fractions during ripening. Physiol Plant **74:** 365–370

Tucker GA, Grierson D (1982) Synthesis of tomato polygalacturonase during fruit ripening. Planta **155:** 64–67

Varner JE, Lin LS (1989) Plant cell wall architecture. Cell **56:** 231–239